Scientia Iranica, Vol. 6, No. 2, pp 75–85
© Sharif University of Technology, April 1999

SCIENTIA
IRANICA

Review Article

Survey, Prediction by a Vortex-Lattice Method, and Measurement for Axial-Flow Ventilation Fans with Sheet-Metal Blades

R.A. Hardin[1] and L.C. Burmeister*

The open literature pertinent to airplane propellers, helicopter rotors, marine propellers and axial-flow fans is surveyed for techniques and information applicable to the prediction of flow about the rotating sheet-metal blades of axial-flow ventilation fans and to the design of these blades. Among these are whole-field computational-fluid-dynamic techniques which provide flow detail, active and passive control of leading-edge separation and vortexes shed from blades and their tips, active means for control of blade shape to maintain fan performance over a range of operating conditions and use of optimization and expert-system techniques. Additionally, the accuracy of a vortex-lattice method is established by comparing predicted with measured power consumption, increase in total pressure and blade surface pressure for an axial-flow ventilation fan with sheet-metal blades.

INTRODUCTION

Recently devised techniques of Computational Fluid Dynamics (CFD) enable computer-aided prediction of fluid flow around rotating fan blades, offering the possibility of improved axial-flow ventilation fan performance over that obtainable with older analysis and design methods [1] which cannot take as many details into account. The blades of these fans are often thin plates, usually stamped from sheet metal. The fan efficiency provided by thin-plate blades can be close enough to that provided by blades of airfoil cross section that the former are the ones of economic choice.

In the following, the open literature pertinent to airplane propellers, helicopter rotors, marine propellers and axial-flow fans is surveyed for techniques and information that are applicable to the analysis and design of axial-flow ventilation fans. Then, the application of a Vortex-Lattice Method (VLM) to predict the performance of an axial-flow ventilation fan with sheet-metal blades is described. Finally, measurements for this fan are compared with the predictions of that VLM.

1. *Department of Mechanical Engineering, University of Iowa, Iowa City, Iowa 52242, USA.*
*. *Corresponding Author, Department of Mechanical Engineering, University of Kansas, Lawrence, KS 66045, USA.*

LITERATURE SURVEY

In contrast to CFD computer programs that are whole-field solvers of the describing Navier-Stokes equations, a VLM only requires determination of velocities and pressures on the blade and solid surfaces at the locations of interest. This advantage led to computer implementations of the VLM for airplane propeller, helicopter rotor and marine propeller applications.

Airplane Propeller

Panel and vortex-lattice, sometimes referred to as lifting-surface, methods are among the boundary element methods used to solve equations that describe inviscid flow [2]. Panel methods were devised by Hess [3] to compute potential flow about a lifting aerodynamic body, primarily for airplane surfaces, extended [4] to higher-order panels and applied [5] to airplane propellers [6]. Source and dipole singularities are utilized on the airfoil blades and concentrated vortex singularities are used to represent the helical wake, predictions that are in good agreement with the measured surface pressures [7].

Helicopter Rotor Blade

The air flow patterns, especially in the hovering state, through the rotor and in the wake of a helicopter (shown in Figure 1) are similar to those of an axial-flow fan, despite the differences in application and, to some extent, in blade solidity. The contraction of the wake is evident in all states except the windmill-brake in which the direction of flow is reversed. Also, two states exhibit recirculation, where some of the air that has passed downward through the rotor quickly returns around the outside of the rotor to be entrained upstream from the inlet. The wake structure of a helicopter rotor is displayed in Figure 2 and it is helpful to recount the processes that lead to it. A blade is a lifting surface, so, vorticity corresponding

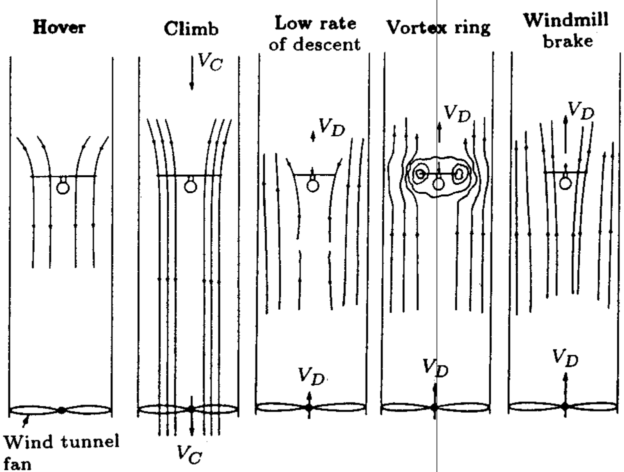

Figure 1. Helicopter vertical flight flow states illustrated by wind tunnel conditions (Prouty [8]).

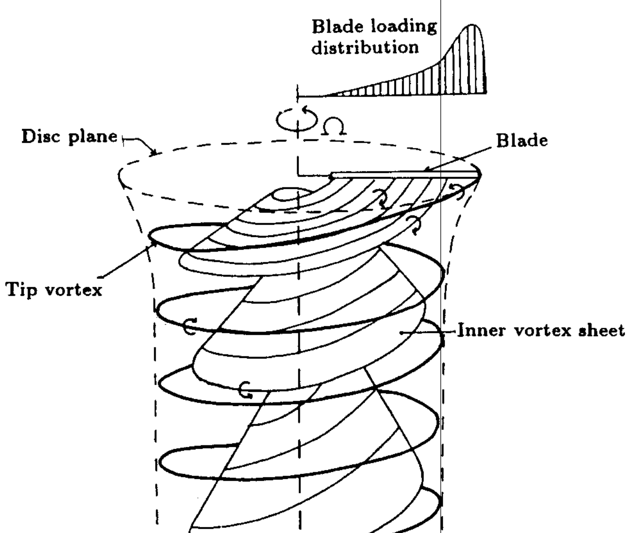

Figure 2. The total wake of a helicopter in hover discerned by smoke flow visualization (Seddon [9] due to Gray [10] and Landgrebe [11]).

to the local lift is generated at all points along the blade span. Corresponding to this bound vorticity, by Helmholtz' theorem, a vortex system must exist in the wake in such a manner that the strength of the wake vortexes is governed by the rate of change of circulation along the blade span. If this rate of change were constant (impossible because of the increase of tangential velocity of a single blade from root to tip), the wake for a single blade in hover would consist of a vortex sheet of constant spanwise strength, descending without contraction. In addition to the bound vortexes, a vortex emanates from the blade tip [12]. In hover, the tip vortex descends below the rotor in a helix, initially moving radially inward toward the axis of rotation. This inward movement gives the succeeding tip an upwash, increasing its effective incidence that intensifies the tip vortex shed from that blade and being responsible for the rapid increase in blade loading past the 80%-span location, as shown in Figure 2. Because the blade loading increases radially, the wake contains an inner vortex sheet that differs from the tip vortex, normally of the opposite sign. The inner sheet moves downstream faster than the tip vortex and the outer part of the sheet moves faster than the inner part so that the helix angle increases in the downstream direction.

In helicopter rotor analysis either a free wake or a prescribed wake assumption is common [13]. The free-wake approach requires an iterative procedure, aligning vortex elements with local velocity in the wake so that they remain force free. The prescribed wake model relies on flow visualization or other measurement techniques to provide parameter values to reproduce rotor wakes.

Helicopter rotor analysis and design has been an important application of CFD techniques [14]. A computationally intensive CFD program is Transient Unsteady Rotor Navier-Stokes (TURNS) that solves thin-layer Navier-Stokes equations for transonic unsteady flows about rotor blades and in the wakes of helicopters [15]. Although good agreement with the measurements was obtained for thrust, the figure of merit predicted with TURNS was 2% under the measured one, no better than the prediction of a VLM which has an order of magnitude lower computational cost. In blade-tip vortex interaction studies, it was found that, because the flow in and near the vortex is highly swirling and turbulent, the accurate turbulence models needed probably were not present in early simulations.

Some findings for helicopter rotors are also of interest for axial-flow ventilation fans. A few wide blades are generally better than numerous narrow blades, since they reduce the power expended for overcoming blade drag at a specified rotational speed, because the vortexes of one blade have time to get out of the way before the next blade passes by. Blade twists in the -8° to -14° range are common; high twist is good for hovering out of the ground effect while low twist is more efficient in the ground effect [11]; a special nonlinear twist (an optimum exists [16]) at the blade tip can reduce blade-tip vortex interference. Nonsquare tips might make the blade load more uniform and reduce the noise generated during passage through the tip vortex of the preceding blade, provided that the tip shape spreads out the tip vortex, making the blade-tip vortex interaction less violent. Backswept tips are advantageous and quieter [17].

To minimize blade-tip vortex interactions, passive means of reducing the strength of the tip vortex have been studied [18,19]. A blade with an Ogee tip has a weaker tip vortex than a rectangular, swept back, or trapezoidal tip blade [20]. Downward-pointing winglets have favorable effects on blade-tip vortex interactions during forward flight [21]. The tip vortex can be located farther away from the blade as a result of using a large anhedral angle in the tip region [22].

Active means of control through leading and trailing edge flaps [23] produce what can be called a smart, or compliant, blade surface; a flap begins to move (either up or down, as appropriate) when a vortex is ahead of the blade and completes its cycle of deflection when the vortex has passed. The efficacy of leading-edge slats has been shown for both axial-flow fans [24] and helicopter rotors [25]. A Gurney flap improves the efficiency of helicopter rotors [26]. Active means of controlling helicopter rotor blade twist (by $\pm 2^\circ$ at the tip) in which active fibers, activated by piezoelectric means, are integrated with the composite material of the blade have been developed [27]. Piezoelectric stacks have been used to power a helicopter rotor trailing edge flap [28]. Active control of wingtip vortex flows has been reported [29].

Marine Propeller

The flows around marine propeller blades and axial-flow fan blades are similar with the exception that cavitation is not a factor in the latter. As reviewed [30], Kerwin and Lee [31] presented a lifting-surface technique to analyze marine propeller performance in both steady and unsteady flow along the lines set forth [3] for aircraft. Later, Greeley and Kerwin [32,33] devised the Propeller Steady Flow-2 (PSF-2) computer program. The PSF-2 program was extended [7] to the prediction of blade surface pressure, consistent with panel-method predictions [5]. Unsteady propeller analysis with the lifting surface technique was implemented [34] in the Propeller Unsteady Force codes PUP-2 and PUP-3 with and without cavitation, respectively, accounting for a prescribed inlet flow field. Unsteady propeller analysis with inclusion of blade thickness effects and cavitation has also been performed [35].

Ducted propellers were treated by Kerwin et al. [36] and Kinnas [37] with the Ducted Propeller Steady Flow (DPSF-2) computer program, using a vortex-lattice treatment of the blade and a panel-method representation of the duct. This ducting is analogous to the Venturi panel that shrouds typical axial-flow ventilation fans, although flow also occurs over the outer surface of the duct of a marine propeller. The DPSF-2 was applied [38] to determine the optimal radial distribution of circulation for ducted propellers with experimental validation [39]; boundary element analysis of unsteady propeller flow was also executed [40]. The Propeller Blade Design family of programs, PBD-10 [33] and PBD-14 [41] for a ducted propulsor, uses a vortex-lattice model to determine the blade shape required to produce a prescribed radial distribution of force loading (or circulation). In the PBD programs at preset operating conditions, an optimal radial circulation distribution can be determined such that the torque is minimized; optimal loading used in a PBD program would give a corresponding optimized blade geometry.

Optimization and Expert System

Blade design is aided by organized methods for adjusting the blade shape to improve performance, including noise generation. In one attempt, a Navier-Stokes solver was used to obtain the effect of leading edge shape on blade performance; parameters of a functional fit to the results were then optimally selected [42]. In another, a genetic algorithm as a global optimizer and a feasible direction technique as a local refining optimizer were used [43]. A VLM for helicopter blade aerodynamic behavior was coupled with an optimization procedure to optimize blade twist, chord, anhedral, sweep etc. [44]. Means for controlling the shape of airfoils that can adapt their shapes to perform optimally under changing conditions have been devised [45].

An inverse method to design airfoil cross sections that meet prescribed surface pressure distributions on a blade and increase thrust or reduce torque has been devised [46]. Expert systems to ascertain fan blade shape, sweep, number and rotational speed that minimize power consumption and noise while meeting pressure rise and flow rate requirements were explored [47-50]. Genetic algorithms have been applied to the optimal design of helicopter rotors, including considerations of noise generation [51-53]. Combined artificial intelligence and numerical optimization systems for automated design of marine propellers [54] and artificial neural networks for the design of turbomachinery airfoils [55] suggest further possibilities.

Axial-Flow Fan

It has been found that axial-flow fans with blades of high sweep and twist can be both more efficient and quieter than those with simpler blade shapes [56-58]. In a test of a ducted contrarotating fan, best performance was obtained with an axial gap of 50% of the first fan chord, serrations on the blades of the second fan and casing boundary layer suction between the two fans [59]. An optical scheme [60] produces an apparently stationary rotor, easing visualization (see Hardin [61] for a survey) of flow relative to a blade.

Measurement and prediction of noise from axial-flow fans have been studied by many researchers [62-65]. Uneven spacing of blades suppresses noise which can be made white if blade spacing and angle are properly chosen [66]. Flow disturbances due to upstream supports and objects can increase the noise of an axial-flow fan; aerodynamic shaping of obstructions, an upstream axial distance of at least 0.3 fan radii for unavoidable obstructions and a baffle to smooth inlet flow are among the measures that reduce noise [67]. Downstream struts have been found to impose a fluctuating pressure on upstream blades [68].

Details of flow about the blades of an axial-flow fan can be obtained by use of commercially available whole-field CFD programs [69]. The effect of forward skewed rotor blades on axial-flow fan performance has been studied [70]; a finite element procedure was used to design automotive radiator fan blades with forward-swept and ringed airfoil blades [71].

An intelligent system for axial-flow fan design was contrived [72]. In the first option, blade-element techniques are used to obtain a preliminary design that meets specifications. In the second option, a data base of previously designed fans is searched for a set of scaled fans that would satisfy the specifications; one of these fans is then refined. As fans are designed and added to the data base, the system learns so that the second option predominates.

A VLM APPLIED TO THIN-PLATE BLADE DESIGN

The PSF-2 computer program [37] was selected for the task of determining the flow about and the forces acting on rotating thin-plate blades of a commercially available axial-flow ventilation fan. In the vortex-lattice method, the flow is assumed to be irrotational and steady with respect to the rotating blade, the fluid is incompressible and inviscid and the flow field is unbounded. The boundaries of a body in such a flow will be streamlines. As a result, a surface in such a flow can be represented by a distribution of singularities, vortexes, on the surface.

Mathematical Description of PSF-2

The essential points of the VLM are the usage of vortex elements and their associated circulation in predicting flow related forces on a surface by means of the Kutta-Joukowski law [73]:

$$L = \rho V \times \Gamma \ , \tag{1}$$

where L is the lifting force per unit span of the airfoil. For a point of differential area δA on a lifting surface where the vorticity strength is γ and the velocity is V, the force δF is:

$$\delta F = \rho V \times \gamma \delta A \ . \tag{2}$$

For a vortex element, the Kutta-Joukowski law gives the force F on an element of length l as:

$$F_i = \rho l_i (V_i \times \Gamma_i) \ , \tag{3}$$

where the subscript i denotes a variable at the location of a vortex element. The velocity and circulation strength are evaluated using the lifting surface equation.

The lifting surface is discretized into panels as illustrated in Figure 3. The spanwise (bound) vortex is at the $\frac{1}{4}$ chord length and the condition of flow tangency is applied at the midspan of the panel at the $\frac{3}{4}$ chord length in a point collocation method [74,75]. In this manner, the predicted circulation equals that given by thin-airfoil theory [76] and the Kutta condition at the trailing edge is satisfied. Vortex-lattice panels are uniformly spaced in the spanwise direction; both the root and the tip lattice elements are inset by a quarter of a panel.

The vorticity distribution of the lifting surface is discretized into a lattice of intersecting straight-line segments. The conservation of vorticity principle is applied to determine the strength of each vortex element, having both free and bound components. By the Biot-Savart law, a vortex element of length L will induce a velocity V according to:

$$V = \frac{\Gamma}{4\pi} \int_L \frac{s \times r}{r^3} dL \ . \tag{4}$$

Here, s is the unit tangent vector along the element, Γ the strength of the vortex element and r the direction vector from the vortex element to the point in the flow at which the velocity is induced. Equation 4 applies to a vortex filament of arbitrary path, usually taken to be a straight line segment for simplicity.

The lifting surface equation results from the condition that the lifting surface is a streamline in the potential flow, requiring that the normal component of the velocity vanishes at the surface. This is formulated by adding the velocity V_r, due to surface vorticity from

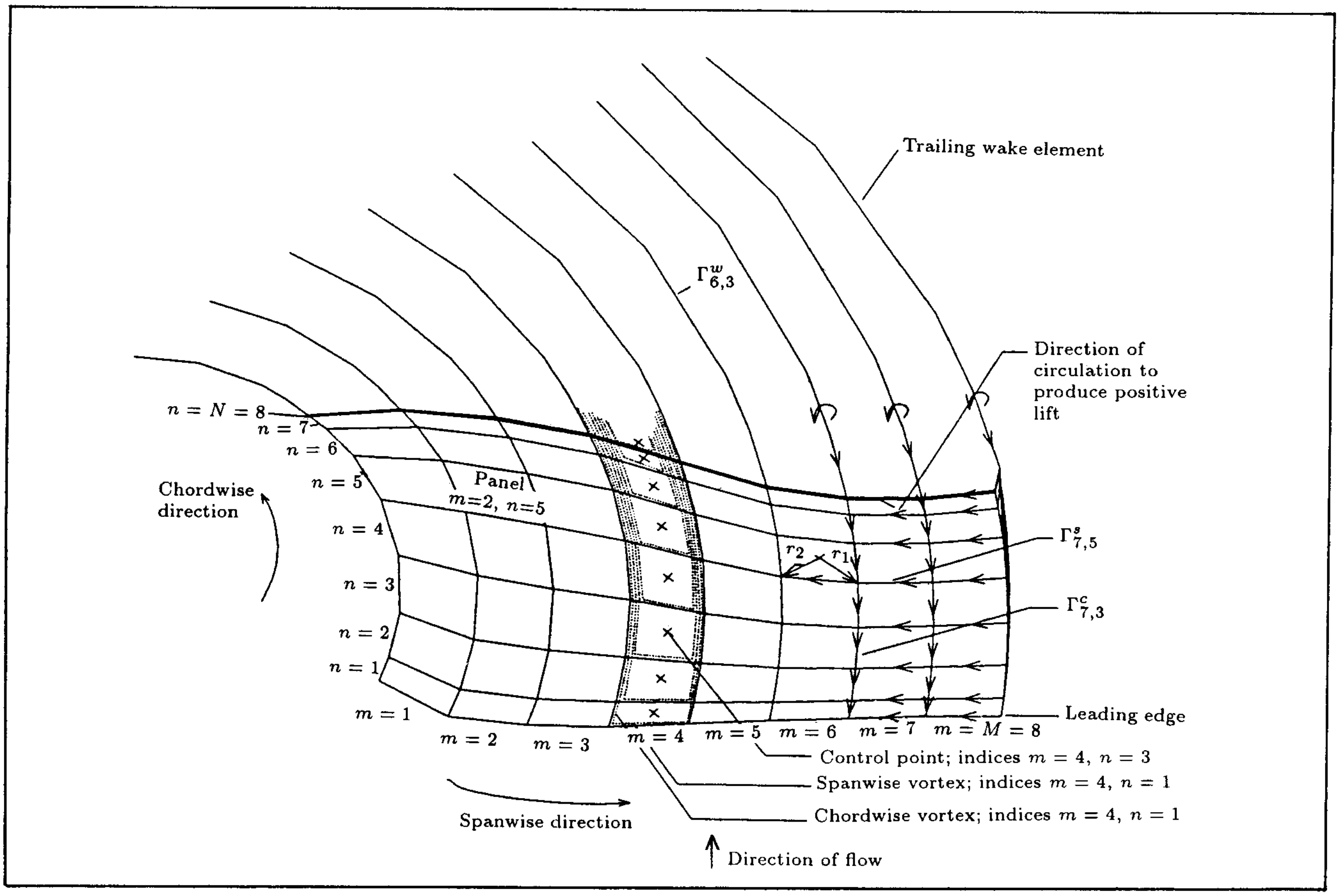

Figure 3. A vortex lattice with vortex element and control point locations indicated [61].

Equation 4, to the onset velocity V_{total}, due to the free stream component and a rotational component, since the problem is solved in a blade-fixed coordinate system, to obtain:

$$[V_r + V_{\text{total}}] \bullet n = [\frac{\Gamma}{4\pi} \int_L \frac{s \times r}{r^3} dL + V_{\text{total}}] \bullet n = 0 \ . \tag{5}$$

The onset flow is composed of axial, radial and tangential components as:

$$V_{\text{total}} = V_a x + V_r r + (V_\theta + \omega r)\theta \ . \tag{6}$$

Equation 6 is satisfied on the lifting surface and the variables solved for on the boundary of the problem specify the solution everywhere.

The discretized form of the lifting surface, Equation 5, is solved at the control point locations on the lifting surface. In doing so, the total normal velocity at the surface at the ith control point is set to zero, giving a system of $M \times N$ equations for the M spanwise and N chordwise control points. The normal velocity at the ith control point is due to a vortex at the m, nth location through an influence coefficient $(A_{m,n})_i$. The discretized form of Equation 5 is summed over all rotor blades to obtain:

$$\sum_{m=1}^{m} \sum_{n=1}^{N} \Gamma^s_{m,n} \Big(\sum_{k=1}^{KBLADE} (A^s_{k,m,n})_i \Big) + \sum_{m=1}^{M+1} \sum_{n=1}^{N} \Gamma^c_{m,n} \Big(\sum_{k=1}^{KBLADE} (A^c_{k,m,n})_i \Big) + \sum_{m=1}^{M+1} \sum_{n=1}^{NWAKE} \Gamma^w_{m,n} \Big(\sum_{k=1}^{KBLADE} (A^w_{k,m,n})_i \Big) + V \bullet n_i = 0 \tag{7}$$

Here the superscripts s, c and w denote spanwise, chordwise and wake elements, respectively, $NWAKE$ is the number of wake elements at spanwise index m, $KBLADE$ is the number of blades and the subscript i indicates evaluation at the ith control point.

Since the wake is stipulated to be force free, an iterative solution procedure is necessary. Induced velocities are computed from the solution to Equation 12 and the wake is aligned according to the new vortex distribution on the blades. Resolution of Equation 12 and realignment of the wake proceeds iteratively until the results converge.

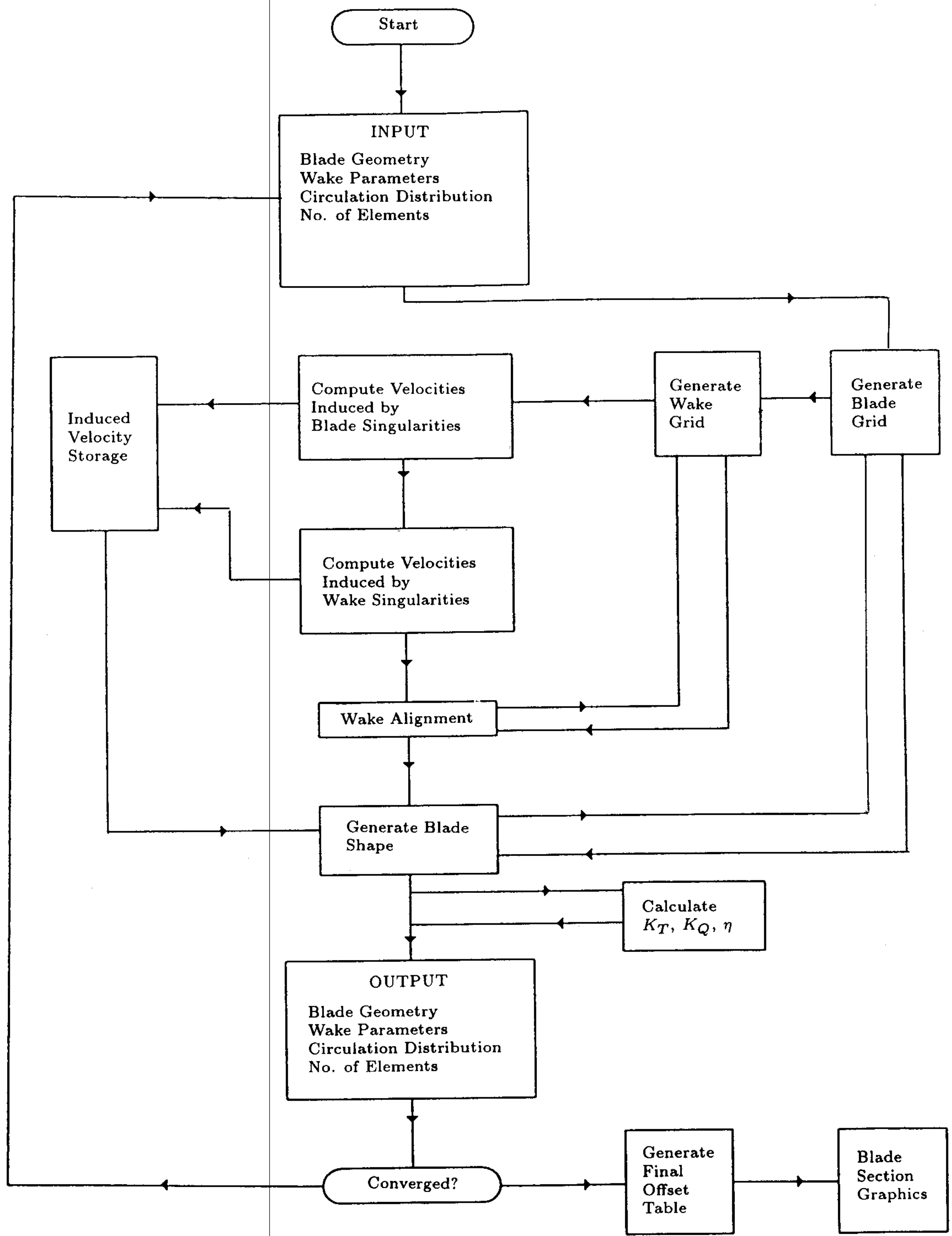

Figure 4. An outline of the PSF-2 analysis computer program [61].

Modifications to PSF-2

The PSF-2 program (see Figure 4), modified by Hardin [61] for this specialized application, was named Fan Steady Flow (FSF). First, a graphical output section was added to ease the demonstration of such flow structures as the wake and tip vortexes. Second, the volumetric flow rate was calculated by integrating the input inlet velocity profile and the increase in total pressure across the fan was calculated as equal to the thrust force divided by the area of the rotor disk. Third, 12 spanwise and 12 chordwise panels and a tip vortex were utilized on each fan blade, rather than having fine discretization and a tip vortex only on the key blade. Fourth, lift versus drag data for flat cambered plate blades were used and a lift coefficient was estimated from the sum of the bound circulations of the radial position of the blade section of interest. Finally, a Venturi panel was represented by panels on each of which there was a vortex whose strength had to be determined and the trailing wake from the Venturi panel extended downstream to the end of the ultimate wake of the rotor.

EXPERIMENTATION

Experiments were performed with an axial-flow ventilation fan (see Figure 5- three blades of 36 in. diameter and 0.06 in. thickness, galvanized steel, vertical direct drive at 850 rpm, poultry fan, model 3C675) manufactured by Lenexa Products and sold by the Dayton Electric Manufacturing Company. This fan is referred to as the LP-36 fan. The fan was mounted on the motor shaft downstream of the two motor-support struts (1.5 in. width, 3 in. separation) welded to the inlet side of a Venturi panel, a 40-in. square piece of deep-draw steel with a 36.5-in.-diameter orifice mounted in a 16-in. deep, 41-in. square wooden crate. Its performance was measured in a fan testing facility certified by the Air Movement and Control Association Inc. (AMCA) in accordance with ANSI/AMCA 210-85 and ANSI/ASHRAE 51-1985 standards.

Blade surface pressures were measured with a SenSym SX01DN (0.1 ms for 10% to 90% of full scale response to a step input, 0 to 1 psi range, unamplified full scale output of 20 mV) pressure transducer-amplifier assembly mounted at the rotor hub. Tygon tubing of 0.092 in. o.d. ran from the low pressure side of the transducer along the trailing edge of a blade and then chordwise on the surface opposite to that on which pressure was to be measured to the pressure tap. The high pressure side of the transducer was open to ambient pressure at the fan rotor hub. The amplified signal was taken to a data acquisition system through mercury-filled slip rings. After acquisition, the pressure signal was corrected for the influences of time lag and amplitude attenuation caused by the Tygon tubing [61,77]. Additional measurements, including flow visualization on the blade surface and in the wake, were made by Hardin [61] to enable assessment of the predictive ability of the FSF program.

PERFORMANCE PREDICTED WITH FSF

The performance of the LP-36 fan was predicted with the FSF program. Numerical values for eight input parameters (six dealing with wake calculation, one a leading edge suction recovery factor and a blade section drag coefficient) for the FSF program were obtained from flow visualization [61] whenever possible.

To improve prediction, a trend study was performed to determine the effect of input parameter values. In this, measured fan performance was compared with the prediction for standard parameter values. Then, one parameter at a time was varied from its baseline value at typical operating conditions (850 rpm and 7,978 cfm), fan efficiency, power and rise in total pressure were plotted versus that parameter. Following this, the parameter value that minimizes the error between prediction and measurement at 850 rpm was determined.

With "tuned" parameter values in hand, fan performance for 600 rpm conditions was predicted, comparing well with measurements as shown in Figure 6.

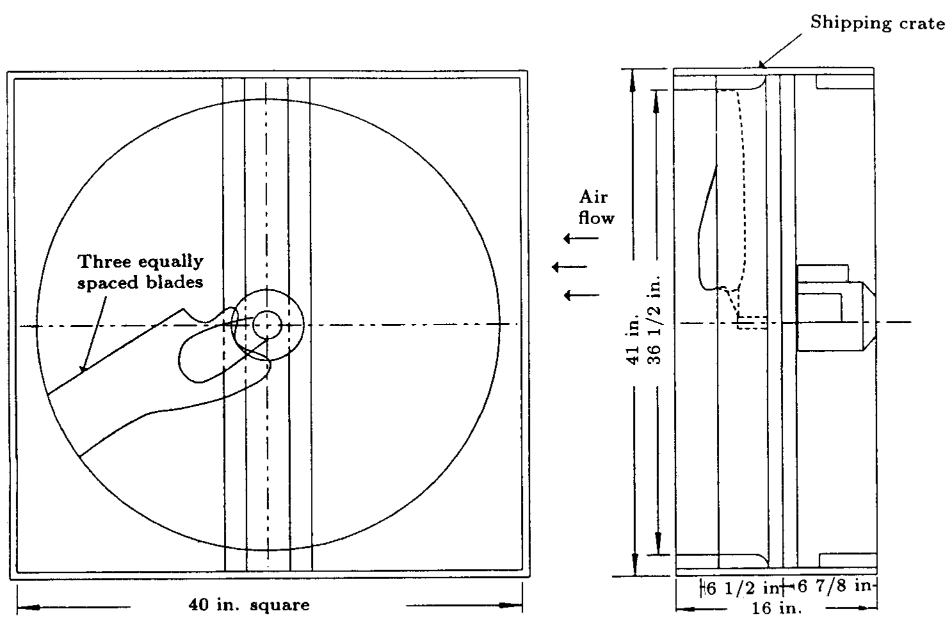

Figure 5. The Lenexa products 36-in.-diameter (LP-36) fan and venturi panel [61].

Without the Venturi panel, power is under predicted by 20-30%; with the Venturi panel, better agreement results. The "after" case incorporates slightly altered parameter values to achieve more accurate predictions. Because small errors in predicted power and rise in total pressure can lead to larger errors in efficiency, the discrepancy between measured and predicted efficiency is not as important as the discrepancies for power and rise in total pressure.

Surface pressures measured on a rotating blade had a fluctuating component. Regions of the lowest blade loading occurred at times during which the blade was in the corners of the packing crate in which the fan was mounted. Separated flow was observed by flow visualization in the locations that corresponded to the times of the pressure peaks. The highest blade loading at the leading edge occurred when the fan was near the side walls of the crate and in the wakes of the motor-support struts, locations where suction-side flow separation was observed.

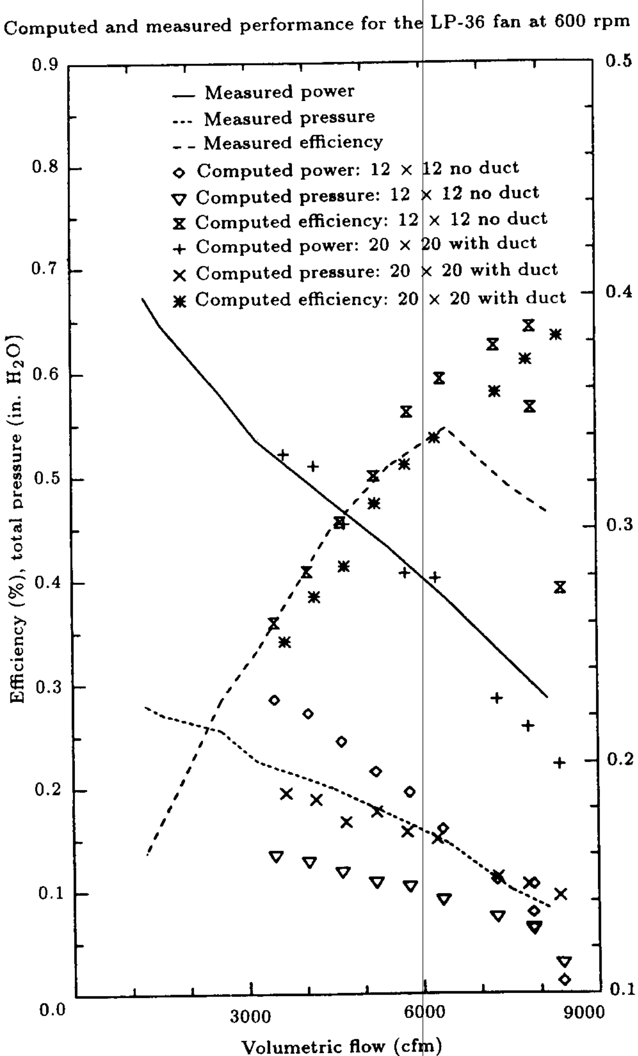

Figure 6. Comparison of measured and FSF-predicted performance of a 600 rpm, LP-36 fan with venturi panel [61].

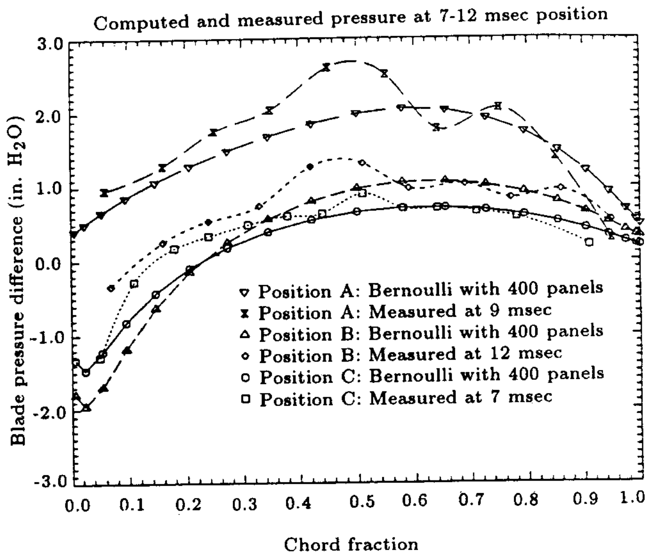

Figure 7. Comparison of measured and FSF-predicted pressure differences on a rotating blade of an LP-36 fan with venturi panel at a blade position neither in a strut wake nor near a packing-crate wall. Positions a, b and c are at 87%, 61% and 43% of the maximum radius, respectively [61].

Surface pressure measurements for blade positions neither in a strut wake nor near a crate wall are shown in Figure 7. The agreement between measured and predicted values suggests that VLM accurately predicts blade loading for uniform flow inlet conditions.

CONCLUSIONS

A survey of the open literature reveals that numerical techniques recently developed for detailed analysis of flow about rotating airplane propellers, helicopter rotors and marine propellers are applicable to axial-flow ventilation fans. Of these, the VLM is well suited to the thin-blade case, especially if economy of computational effort is a consideration. Whole-field CFD techniques, however, can also be successful, either from the beginning or as refiners of solutions rapidly obtained with a VLM. Means of controlling separation, vortexes shed from blades and their tips and blade shape might be applied to improve fan performance. Optimization and expert-system techniques might be adapted to speed up the design of improved fans.

REFERENCES

1. Wallis, R., *Axial Flow Fans and Ducts*, Wiley, New York (1983).

2. Anderson, J., *Fundamentals of Aerodynamics*, McGraw-Hill (1984).

3. Hess, J. "The problem of three-dimensional lifting potential flow and its solution by means of surface singularity distribution", *Computer Methods in Applied Mechanics and Engineering*, **4**, pp 283-319 (1974).
4. Hess, J. "The use of higher-order surface singularity distributions to obtain improved potential flow solutions for two-dimensional lifting airfoils", *Computer Methods in Applied Mechanics and Engineering*, **5**, pp 11-33 (1975).
5. Hess, J. and Valarezo, W. "Calculation of steady flow about propellers using a surface panel method", *AIAA J. of Propulsion*, **1**, pp 470-476 (1985).
6. Hess, J. "Panel methods in computational fluid dynamics", *Annual Review of Fluid Mechanics*, **22**, pp 255-274 (1990).
7. Kim, K. and Kobayashi, S. "Pressure distribution on propeller blade surface using numerical lifting-surface theory", *Proc. SNAME Symposium-Propellers 84*, Virginia Beach, Virginia (1984).
8. Prouty, R., *Helicopter Performance, Stability and Control*, Robert E. Krieger Publishing Co., Malabar, Florida, Figure 2.1, p 94 (1990).
9. Seddon, J., *Basic Helicopter Aerodynamics*, American Institute of Aeronautics and Astronautics (1990).
10. Gray, R. "An aerodynamic analysis of a single-bladed rotor in hovering and low speed forward flight as determined from smoke studies of the vorticity distribution in the wake", Princeton University, Aeronautical Engineering Report 356 (1956).
11. Landgrebe, A. "The wake geometry of a hovering helicopter rotor and its influence on rotor performance", *J. of the American Helicopter Soc.*, October, pp 3-15 (1972).
12. Rule, J. and Bliss, D. "Prediction of viscous trailing vortex structure from basic loading parameters", *AIAA J.*, **36**, pp 208-218 (1998).
13. Gray, R. "Vortex modeling for rotor aerodynamics-the 1991 Alexander A. Nikolsky lecture", *J. American Helicopter Soc.*, **37**(1), pp 3-14 (1992).
14. Sankar, L. and Malone, J. "Modern computational methods for rotorcraft applications", in *Computational Fluid Dynamics Techniques*, W. Habashi and M. Hafez, Eds., Gordon & Breach Publishers, pp 47-67 (1995).
15. Wake, B. and Baeder, J. "Evaluation of a Navier-Stokes analysis method for hover performance prediction", *J. American Helicopter Soc.*, **41**, pp 7-17 (1996).
16. Chattopadhyay, A., McCarthy, T. and Pagaldipti, N. "Multilevel decomposition procedure for efficient design optimization of helicopter rotor blades", *AIAA J.*, **33**, pp 223-230 (1995).
17. Prieur, J., Lafon, P., Caplot, M. and Desopper, A. "Aerodynamics and acoustics of rectangular and swept rotor blade tips", *J. American Helicopter Soc.*, **34**, pp 42-51 (1989).
18. Spivey, W. and Morehouse, G. "New insights into the design of swept-tip rotor blades", *26th Annual National Forum of the American Helicopter Soc.* (1970).
19. Carlin, G., Dadone, L. and Spencer, R. "Results of an experimental investigation of blade tip vortex modification devices", NASA CR-181853 (June, 1989).
20. Smith, D. "Helicopter rotor tip shapes for reduced blade vortex interaction - An experimental investigation", AIAA Paper 95-0192, *33rd Aerospace Sciences Meeting and Exhibit*, Reno, NV (Jan. 9-12, 1995).
21. Müller, R., Mba, M., Aymard, D., Favier, D., Berton, E. and Maresca, C. "Visualization and measurement of helicopter rotor flow with swept back tip shapes at hover flight using the 'flow visualization gun' time line technique", *Experiments in Fluids*, **21**, pp 161-169 (1996).
22. Desopper, A., Lafon, P. and Prieur, P. "Effect of an anhedral sweptback tip on the performance of a helicopter rotor", *Vertica*, **12**, pp 345-355 (1988).
23. Hassan, A., Sankar, L. and Tadghighi, H. "Effects of leading and trailing edge flaps on the aerodynamics of airfoil/vortex interactions", *J. American Helicopter Soc.*, **39**, pp 35-46 (1994).
24. Javur, M., Murthy, K. and Kar, S. "The introduction of leading edge slats to improve the off-design performance of axial flow fans", *Papers Presented at the International Conference on Fan Design and Applications, BHRA Fluid Engineering*, Guilford, England, pp 281-294 (1982).
25. Bangalore, A. and Sankar, S. "Numerical analysis of aerodynamic performance of rotors with leading edge slats", Paper AIAA-95-1888-CP, *Proc. 13th AIAA Applied Aerodynamics Conf.*, San Diego, CA, Pt. 2, pp 1013-1023 (June 19-22, 1995).
26. Kentfield, J. "The potential of Gurney flaps for improving the aerodynamic performance of helicopter rotors", AIAA Paper 93-4883, *Proc. AIAA International Powered Lift Conf.*, Santa Clara, CA, pp 283-292 (Dec. 1-3, 1993).
27. Rodgers, J., Hagood, N. and Weems, D. "Design and manufacture of an integral twist-actuated rotor blade", AIAA Paper 97-1264, *38th AIAA/ASME/ASCE/AHS/ASC Structures, Structural Dynamics, and Materials Conference and Exhibit*, Kissimmee, FL (April 7-10, 1997).
28. Spencer, B. and Chopra, I. "Design and testing of a helicopter trailing edge flap with piezoelectric stack actuators", *Proc. Smart Structures and Integrated Systems Meeting*, San Diego, CA, Smart Structures and Materials (Soc. Photo-Optical Instrumentation Engineers Proc., **2717**, pp 120-131 (Feb. 26-29, 1996).
29. Mattewson, C. and Vaklii, A. "Active control of wingtip vortex flows", Paper AIAA-98-0318, *Proc. AIAA 36th Aerospace Sciences Meeting and Exhibit*, Reno, NV (Jan. 12-15, 1998).
30. Kerwin, J. "Marine propellers", *Annual Review of Fluid Mechanics*, **18**, pp 367-403 (1989).
31. Kerwin, J. and Lee, C. "Prediction of steady and unsteady marine propeller performance by a numerical lifting-surface theory", *Trans. SNAME*, **86**, pp 218-253 (1978).

32. Greeley, D. "Marine propeller blade tip flows", MIT Department of Ocean Engineering Report 82-3, Cambridge, MA (1982).

33. Greeley, D. and Kerwin, J. "Numerical methods for propeller design and analysis in steady flow", *Trans. SNAME*, **90** (1982).

34. Lee, C. "Prediction of steady and unsteady performance of marine propellers with or without cavitation by numerical lifting surface theory", Ph.D. Thesis, Massachusetts Institute of Technology (May, 1979).

35. Fine, N. "Nonlinear analysis of cavitating propellers in nonuniform flow", Ph.D. Thesis, Massachusetts Institute of Technology (May, 1992).

36. Kerwin, J., Kinnas, S., Lee, J. and Shih, W. "A surface panel method for the hydrodynamic analysis of ducted propellers", *Trans. SNAME*, **95** (1987).

37. Kinnas, S. "Ducted propeller steady flow", MIT-DPSF2, User's Manual, Department of Ocean Engineering Report, Massachusetts Institute of Technology, 77 Massachusetts Avenue, Cambridge, MA 02139 (1989).

38. Kinnas, S. and Coney, W. "On the optimum ducted propeller loading", *SNAME Symposium-Propellers*, **88** (1988).

39. Hughes, M., Kinnas, S. and Kerwin, J. "Experimental validation of a ducted propeller analysis method", *ASME J. Fluids Engineering*, **114**, pp 214-219 (1992).

40. Kinnas, S. and Hsin, C. "Boundary element method for the analysis of the unsteady flow around extreme propeller geometries", *AIAA J.*, **30**(3), pp 688-696 (1992).

41. Black, S., Egnor, D., Keenan, D., Kerwin, J. and Taylor, T. "PBD-14.1: A coupled lifting-surface design/analysis code for marine propulsors", Department of Ocean Engineering, Technical Report 95-7, Massachusetts Institute of Technology (Feb., 1996).

42. Nakadate, M. and Obukata, M. "Design of new generation rotor blade airfoils using Navier-Stokes", *Proc. 20th European Rotorcraft Forum*, Amsterdam, Netherlands, **2**, pp 33-1 - 33-15 (Oct. 4-7, 1994).

43. Rocchetto, A. and Poloni, C. "A hybrid numerical optimization technique based on genetic and feasible direction algorithms for multipoint helicopter rotor blade design", *Proc. 21st European Rotorcraft Forum*, St. Petersburg, Russia, **1**, pp II.7.1-II.7.19 (Aug. 30-Sept. 1, 1995).

44. Quackenbush, R., Boschitsch, A. and Wachspress, D. "Rotor design optimization using a free wake analysis", NASA-CR-177612 (1993).

45. Austin, F., Rossi, M., Van Nostrand, W., Knowles, G. and Jameson, A. "Static shape control for adaptive wings", *AIAA J.*, **32**, pp 1895-1901 (1994).

46. Tapia, F., Sankar, L. and Schrage, D. "An inverse aerodynamic design method for rotor blades in forward flight", *Proc. 51st Annual AHS Forum*, Fort Worth, TX, pp 893-904 (May 9-11, 1995).

47. Tong, S. "Design of aerodynamic bodies using artificial intelligence/expert system technique", Paper AIAA-85-0112 (1985).

48. Andrews, A. "Progress and challenges in the application of artificial intelligence to computational fluid dynamics", *AIAA J.*, **26**, pp 40-46 (1988).

49. Wesly, L. and Rodman, L. "Toward an integrated CFD expert system environment", *Proc. AIAA 36th Aerospace Sciences Meeting and Exhibit*, Reno, NV, AIAA Paper AIAA-98-1005 (Jan. 12-15, 1998).

50. Hamilton, J., Clarkson, P., Burgess, S. and Newland, D. "The development of a knowledge based system to aid helicopter rotor blade design", *Proc. 20th ICAS Congress*, Naples, Italy, **1**, pp 619-630 (Sept. 8-13, 1996).

51. Wells, V., "Genetic algorithms in conceptual design of a light-weight, low-noise, tilt-rotor aircraft", NASA-CR-201404 (1996).

52. Lee, J. and Hajela, P. "Parallel genetic algorithm implementation in multidisciplinary rotor blade design", *J. of Aircraft*, **33**, pp 962-969 (1996).

53. Quagliarella, D. and Vicini, A. "Hybrid multiobjective genetic algorithm for fluid dynamic design", AIAA Paper AIAA-98-1008, *Proc. AIAA 36th Aerospace Sciences Meeting and Exhibit*, Reno, NV (Jan. 12-15, 1998).

54. Hambric, S., Dai, C., Mulvihill, L., Tong, S. and Powell, D. "A prototype artificial intelligence driven marine propulsor design tool", *5th AIAA/USAF/NASA/ISSMO Symposium on Multidisciplinary Analysis and Optimization*, Panama City Beach, FL, Pt. 1, pp 334-343 (Sept. 7-9, 1994).

55. Rai, M. and Madavan, N. "Application of artificial neural networks to the design of turbomachinery airfoils", AIAA Paper AIAA-98-1003, *Proc. AIAA 36th Aerospace Sciences Meeting and Exhibit*, Reno, NV (Jan. 12-15, 1998).

56. Brown, N. "The use of skewed blades for ship propellers and truck fans", *Noise and Fluids Engineering*, Ed., R. Hickling, pp 201-207 (1977).

57. Wei, J. and Zhong, F. "The effect of forward skewed rotor blades on aerodynamic and aeroacoustic performance of axial-flow fans", AIAA Paper 88-3783-CP, *AIAA/ASME/SIAM/APS 1st National Fluid Dynamics Conference*, pp 1983-1990 (1988).

58. Wright, T. and Simmons, W. "Blade sweep for axial-flow fans", *ASME J. Turbomachinery*, **112**, pp 151-158 (1990).

59. Roy, B., Ravibabu, K., Srinivasan, R., Basu, S., Raju, A. and Murthy, P. "Flow studies in ducted twin-rotor contra-rotating axial flow fans", ASME Paper 92, *Proc. 37th ASME International Gas Turbine and Aeroengine Congress and Exposition*, Cologne, Germany, (June 1-4, 1993).

60. Wu, J., Pullum, L., Welsh, M. and Yunken, R. "Investigation of the relative flow field of an axial agitator

impeller using a combined image shifting and derotation technique", *Proc. ASME Fluids Engineering Division Summer Meeting*, **239**(4), pp 655-660 (1996).

61. Hardin, R. "Analysis of axial-flow ventilation fans by vortex lattice method", Ph.D. Thesis, University of Kansas, Lawrence, KS 66045 (1994).
62. Ohtsuta, K. and Akishita, S. "Noise reduction of shortly ducted fan by using forward swept and inclined blade", AIAA Paper 90-3986, *Proc. 13th AIAA Aeroacoustics Conference*, Tallahassee, FL (Oct. 22-24, 1990).
63. Lee, C., Chung, M. and Kim, Y.-H. "A prediction model for the vortex shedding noise from the wake of an airfoil or axial flow fan blades", *J. Sound and Vibration* (1993).
64. Carolus, T., Fuest, T. and Beiler, M. "Broad band noise prediction of low pressure axial fans employing CFD-flow field data", *Proc. 1st CEAS/AIAA Joint Aeroacoustics Conf.*, Munich, Germany, **1**, pp 151-156 (June 12-15, 1995).
65. Lee, S. and Jin, S.-H. "An experimental study of flow structure in small cooling fans using acoustic similarity", *Turbomachinery Noise, Proc. ASME Noise Control & Acoustics Div. (ASME IMECE, Nov. 12-17, San Francisco, CA)*, **NCA-Vol. 21**, pp 3-9 (1995).
66. Akaike, S., Kikuyama, K., Kitada, M., Kuwayama, K. "Study of rotational noise reduction for axial flow fan", *JSME Int. J., Ser. B*, **39**, pp 550-596 (1996).
67. Washburn, K. and Lauchle, G. "Effects of inflow conditions on discrete frequency noise generated by small axial-flow fans", Report No. AD-A160579; PSU/ARL/TR-85-001, Applied Research Lab., Pennsylvania State University, University Park, PA (1985).
68. Ng, W., Obrien, W. and Olsen, T. "Experimental investigation of unsteady fan flow interaction with downstream struts", AIAA Paper 86-1870, *Proc. 10th AIAA Aeroacoustics Conference*, Seattle, WA (July 9-11, 1986).
69. Matus, R. and Lounsbury, R. "An unstructured grid flow solver for turbomachinery flows", AIAA Paper 93-1913, *Proc. 29th AIAA/SAE/ASME/ASEE Joint Propulsion Conference and Exhibit*, Monterey, CA, (June 28-30, 1993).
70. Jun, W. and Fangyuan, Z. "The effect of forward skewed rotor blades on the aerodynamic and aeroacoustic performance of axial-flow fans", AIAA Paper 88-3783-CP (1988).
71. Dhaubhadel, M., Akay, H. and Charles, H. "Three-dimensional finite element analysis for aerodynamic design of fan blades", *Proc. AIAA/ASME/SIAM/APS 1st National Fluid Dynamics Congress*, Cincinnati, OH, Pt. 3, pp 1608-1614 (July 25-28, 1988).
72. Jackson, D. and Wright, T. "An intelligent/learning axial fan design system", ASME Paper 91-GT-27, *Proc. 36th ASME International Gas Turbine and Aeroengine Congress and Exposition*, Orlando, FL (June 3-6, 1991).
73. Panton, R., *Incompressible Flow*, Wiley (1984).
74. Lan, C., *Applied Wing and Airfoil Theory*, Cheng Chung Book Co., Taipei, Taiwan (1988).
75. Lan, C. "A quasi-vortex lattice method in thin wing theory", *J. Aircraft*, **11**, pp 518-527 (1974).
76. James, R. "On the remarkable accuracy of the vortex-lattice method", *Computer Methods in Applied Mechanics and Engineering*, **1** (1972).
77. Hardin, R. and Burmeister, L. "Unsteady surface pressure measurement on a rotating axial-flow fan blade", ASME Paper 94-WA/HT-18 (1994).